

Proceedings Article

Rapid relaxation-based color MPI

M. T. Arslan^{1,2,*}, S. Kurt^{1,2}, A. A. Ozaslan^{1,2}, Y. Muslu^{1,3}, E. U. Saritas^{1,2,4}

¹Department of Electrical and Electronics Engineering, Bilkent University, Ankara, Turkey

²National Magnetic Resonance Research Center, Bilkent University, Ankara, Turkey

³Department of Biomedical Engineering, University of Wisconsin-Madison, Madison, WI, USA

⁴Neuroscience Program, Sabuncu Brain Research Center, Bilkent University, Ankara, Turkey

*Corresponding author, email: mtarslan@ee.bilkent.edu.tr

© 2020 Arslan *et al.*; licensee Infinite Science Publishing GmbH

This is an Open Access article distributed under the terms of the Creative Commons Attribution License (<http://creativecommons.org/licenses/by/4.0>), which permits unrestricted use, distribution, and reproduction in any medium, provided the original work is properly cited.

Abstract

Color magnetic particle imaging (MPI) techniques have recently gained popularity, with the purposes of distinguishing different nanoparticle types or nanoparticles in different environments. In this work, we extend a relaxation-based color MPI technique that we recently proposed, and make it applicable to rapid trajectories that distort the underlying mirror symmetry of the adiabatic MPI signal. We propose a method to recover the mirror symmetry, with delay and signal amplitude compensations. The proposed technique rapidly produces a relaxation map of the scanned region, without any prior information about the nanoparticles.

I Introduction

Color magnetic particle imaging (MPI) techniques have recently gained interest [1], with potential applications of catheter tracking during cardiovascular interventions [2], tracking of drugs carried by nanocarriers [3], and identifying characteristics of local environment such as temperature and viscosity [4-7]. Color MPI has been realized with both system function reconstruction and x-space approaches. Previously, we have proposed an x-space-based color MPI technique, where the relaxation time constant, τ , is estimated in a calibration-free fashion. This technique, called TAURUS (TAU estimation via Recovery of Underlying mirror Symmetry), was previously demonstrated for a trajectory where the partial field-of-view (pFOV) center was moved to discrete positions.

In this work, we extend TAURUS to rapid trajectories that continuously move the pFOV center. We first show the distortion in mirror symmetry of the adiabatic MPI signal caused by a rapid trajectory, and propose a technique to recover the mirror symmetry. With simulations and experimental results, we show that the proposed

technique can rapidly and successfully distinguish different nanoparticle types, without any prior information.

II Materials and Methods

II.1 Theory

For a drive field (DF) applied simultaneously with a linearly ramping focus field along the z-axis, the field free point (FFP) trajectory can be expressed as:

$$x_s(t) = \frac{B_p}{G_z} \cos(2\pi f_d t) + \frac{R_s}{G_z} t \quad (1)$$

Here, B_p (T) is the DF amplitude, f_d is the DF frequency, G_z (T/m) is the selection field gradient along the z-axis, and R_s (T/s) is the focus field slew rate. This trajectory moves the FFP at a constant speed $R = R_s/G_z$, while the drive field rapidly moves the FFP back and forth.

Figure 1 shows the FFP movement for $R_s = 20$ T/s and the corresponding adiabatic signal (i.e., signal without relaxation effects) for the case of a point source sample.

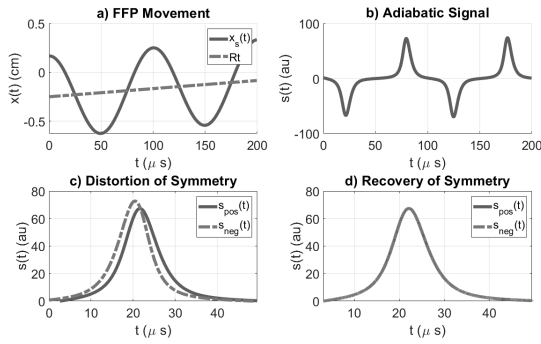


Figure 1: (a) FFP movement and (b) adiabatic MPI signal for a rapid trajectory with $R_s = 20$ T/s. (c) Distortion and (d) recovery of mirror symmetry.

The constant speed along the z-axis causes a delay between negative/positive signals (i.e., signals from negative/positive scanning directions), as well as a mismatch in signal amplitudes. The resulting distortion of the underlying mirror symmetry needs to be compensated before TAURUS can be utilized with a rapid trajectory.

A closed form expression for the additional delay, Δt , caused by the constant FFP speed can be found by solving the following equation:

$$x_s(t_0) = x_s(t_0 + T/2 + \Delta t) \quad (2)$$

where

$$t_0 = \operatorname{argmax}_t |\dot{x}_s(t)|, \quad 0 < t < T/2 \quad (3)$$

Accordingly, Δt represents the delay in FFP motion for the central position of the pFOV during back and forth scanning. Equation 2 can be solved via Taylor series expansion of $x_s(t)$ in Eq. 1. Next, the mismatch in signal amplitudes at pFOV center can be compensated by using FFP speed at pFOV center during negative/positive scanning, i.e., $\dot{x}_s(t_0)$ and $\dot{x}_s(t_0 + T/2 + \Delta t)$. Note that Δt depends on B_p , G_z , R_s , and f_d . Figure 1 shows an example of this correction for a high slew rate of $R_s = 20$ T/s, where mirror symmetry is recovered successfully.

II.II Simulations

Simulations were performed in MATLAB using a custom MPI toolbox. To match the experimental conditions, selection field gradients were chosen as $(-4.8, 2.4, 2.4)$ T/m, with $B_p = 10$ mT and $f_d = 10$ kHz DE, and 25-nm nanoparticle diameter. Relaxation effects were incorporated using the model in [10]. First, a point source was placed at the center of the field-of-view (FOV) with $\tau = 2 \mu\text{s}$. Signal-to-noise ratio (SNR) robustness of the proposed method was evaluated for SNR ranging between 1-20, and R_s ranging between 1-20 T/s. Simulations were repeated 1000 times for each case and normalized root-mean-squared error (nRMSE) of τ estimations (i.e., error

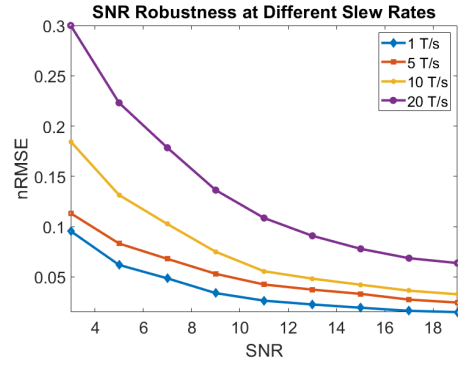


Figure 2: SNR robustness of the proposed technique.

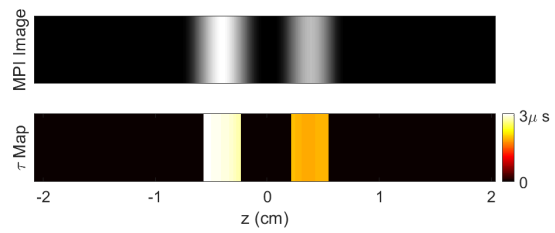


Figure 3: Simulation results for two different nanoparticles with $\tau_1 = 3 \mu\text{s}$ and $\tau_2 = 2 \mu\text{s}$, placed at 7.8-mm separation. The peaks of the estimated values were $\tau_1 = 2.98 \mu\text{s}$ and $\tau_2 = 1.92 \mu\text{s}$. 1D results are replicated and stacked vertically in a pseudo-2D image format for visual display.

normalized by the actual τ) were computed. Next, two different nanoparticles with Gaussian spatial distributions of $\sigma_1 = 0.1$ mm with $\tau_1 = 3 \mu\text{s}$ and $\sigma_2 = 0.8$ mm with $\tau_2 = 2 \mu\text{s}$ were placed at a 7.8-mm separation. This second simulation used a linear trajectory with $R_s = 1$ T/s.

II.III Imaging Experiments

Experiments were performed on our in-house MPI scanner with $(-4.8, 2.4, 2.4)$ T/m selection field gradients. DF parameters were $B_p = 10$ mT and $f_d = 9.7$ kHz. A robot arm with constant speed was utilized instead of a focus field. This linear motion was used at its maximum speed of $R = 2.91$ cm/s along the z-direction, corresponding to $R_s = 70$ mT/s. The total scan time was 3 seconds. A phantom containing three different samples were prepared using Nanomag-MIP (Micromod GmbH) with 1.43 mg Fe/mL, undiluted Vivotrax (Magnetic Insight Inc.) with 5.5 mg Fe/mL, and a homogeneous mixture of the two. These samples were positioned at 1.5-cm separations.

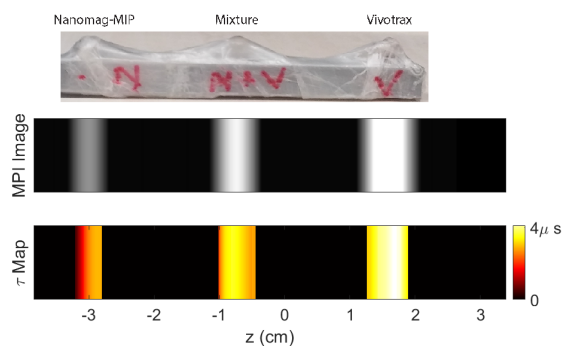


Figure 4: Imaging experiment results for Nanomag-MIP, Vivotrax, and a homogeneous mixture of the two. 1D results are replicated and stacked vertically in a pseudo-2D image format.

III Results

III.I Simulation Results

Figure 2 shows nRMSE for τ estimation at different SNR and slew rates. For SNR > 10, the error in τ estimation remains below 10 % at all tested slew rates, and remains below 5 % for $R_s < 10$ T/s. Figure 3 shows the results for two different nanoparticles placed at 7.8 mm separation, distinguished clearly in the τ map. The τ values were estimated as $\tau_1 \approx 2.98 \mu\text{s}$ and $\tau_2 \approx 1.92 \mu\text{s}$, showing excellent agreement with the actual values.

III.II Imaging Experiment Results

Figure 4 shows the results of the imaging experiments. With a total scan time of 3 seconds and without any prior calibration, Nanomag-MIP, Vivotrax, and their homogeneous mixture were distinguished clearly in the τ map. The peaks of the estimated τ values were $2.87 \mu\text{s}$, $4.2 \mu\text{s}$, and $3.3 \mu\text{s}$, respectively.

IV Conclusions

In this work, we have successfully extended TAURUS to rapid linear trajectories that continuously move the FFP.

While these trajectories distort the underlying mirror symmetry of the adiabatic MPI signal, we show that mirror symmetry can be recovered with delay and signal amplitude compensations. The proposed technique rapidly produces a τ map of the scanned region, without any prior information about the nanoparticles.

Author's Statement

This work was supported by the Scientific and Technological Research Council of Turkey (No. TUBITAK 115E677).

References

- [1] J. Rahmer et al. "First experimental evidence of the feasibility of multi-color magnetic particle imaging." *Phys Med Biol*, vol. 60, no. 5, pp. 1775, 2015.
- [2] J. Rahmer et al. "Interactive magnetic catheter steering with 3-D real-time feedback using multi-color magnetic particle imaging." *IEEE Trans Med Imaging*, vol. 36, no. 7, pp. 1449, 2017
- [3] A. M. Rauwerdink and J. B. Weaver. "Measurement of molecular binding using the Brownian motion of magnetic nanoparticle probes." *App Phys Lett*, vol. 96, no. 3, pp. 033702, 2010.
- [4] T. Viereck et al. "Dual-frequency magnetic particle imaging of the Brownian particle contribution," *J Magn Magn Mater*, vol. 427, pp. 156, 2017.
- [5] A. M. Rauwerdink and J. B. Weaver. "Viscous effects on nanoparticle magnetization harmonics." *J Magn Magn Mater*, vol. 322, no. 6, pp. 609, 2010.
- [6] M. Möddel et al., "Viscosity quantification using multi-contrast magnetic particle imaging," *New Journal of Physics*, vol. 20, no. 8, pp. 083001, 2018.
- [7] M. Utkur et al. "Relaxation-based color magnetic particle imaging for viscosity mapping," *App Phys Lett*, vol.115, no.15, pp. 152403, 2019.
- [8] D. Hensley, et al. "Preliminary experimental X-space color MPI." *Proc of 5th International Workshop on Magnetic Particle Imaging (IWMPI)*, Istanbul, Turkey, 2015.
- [9] Y. Muslu et al. "Calibration-free relaxation-based multi-color magnetic particle imaging." *IEEE Trans Med Imaging*, vol. 37, no. 8, pp. 1920, 2018.
- [10] L. R. Croft et al., "Relaxation in x-space Magnetic Particle Imaging," *IEEE Trans Med Imaging*, vol.31, no.12, pp. 23342, 2012.